Continuous-time random walks: Simulation of continuous trajectories

D. Kleinhans and R. Friedrich
Westfälische Wilhelms-Universität Münster, Institut für Theoretische Physik, D-48149 Münster, Germany
(Received 21 July 2007; published 4 December 2007)

Continuous-time random walks have been developed as a straightforward generalization of classical random-walk processes. Some ten years ago, Fogedby introduced a continuous representation of these processes by means of a set of Langevin equations [H. C. Fogedby, Phys. Rev. E **50**, 1657 (1994)]. The present work is devoted to a detailed discussion of Fogedby's model and presents its application for the robust numerical generation of sample paths of continuous time random-walk processes.

DOI: 10.1103/PhysRevE.76.061102 PACS number(s): 05.40.Fb, 45.10.Hj, 02.60.Cb

I. INTRODUCTION

The extensive analysis of stochastic processes by Bachelier, Einstein, and Langevin [1–3] has inspired scientist in the last century. First, Fokker-Planck equations describing the time evolution of probability density functions (PDFs) emerged. In addition, mathematical methods for proper interpretation of the associated Langevin equations have been developed that allow access to the trajectories of individual particles. An intrinsic feature of these processes is that they obey Markov properties [4]. Therefore, two point statistics are sufficient for a complete description of these processes.

In recent years, processes exhibiting anomalous diffusion, $\langle x^2(t)\rangle \sim t^{\xi}$ with $\xi \neq 1$, increasingly have attracted attention [5]. Such processes typically are realized in complex environments such as porous and disordered media, see, e.g., Ref. [6] and references therein. In contrast to ordinary diffusion, Markov properties do not hold for these processes. Therefore, multipoint joint statistics have to be considered for a proper description of the dynamics. Likewise, two alternative approaches to these processes have been evolved. On the one hand, these processes can be described by means of fractional Fokker-Planck equations that contain fractional derivatives with nonlocal character. On the other hand, continuous-time random-walk (CTRW) processes [7] have been proposed for the analysis of the microscopic properties of anomalous diffusion processes [8]. In general, they are specified by the iterative discrete equations [5,9]

$$x_{i+1} = x_i + \eta_i, \tag{1a}$$

$$t_{i+1} = t_i + \tau_i, \tag{1b}$$

where (η_i, τ_i) is a set of random numbers drawn from the PDF $\Psi(\eta,\tau)$, that vanishes for negative values of τ for reasons of causality. Frequently, Eqs. (1) are used to model time-continuous processes with the additional assignment [7,9]

$$x(t) = x_i, \quad \text{with} \quad t_i \le t < t_{i+1}. \tag{2}$$

With the aid of CTRWs, limiting behavior and ensemble statistics of anomalous diffusion processes become accessible through Monte Carlo simulations. For details, the reader is referred to recent works by Dentz *et al.* [6], Heinsalu *et al.* [10], and Gorenflo *et al.* [11].

Recently, Fogedby formulated a *continuous* description of CTRWs that is based on a set of stochastic differential equations [12],

$$\frac{dx}{ds} = F(x) + \eta(s), \tag{3a}$$

$$\frac{dt}{ds} = \tau(s). \tag{3b}$$

Here, the discrete variable i of Eqs. (1) is generalized to the continuous variable s that can be associated with an intrinsic time of the CTRW. A number of publications addressed statistical properties of trajectories of this approach [13–15]. It is the aim of the present work to present a robust algorithm for the generation of *continuous* sample paths from Fogedby's equations. By this means trajectories can be obtained that properly exhibit the anomalous dynamics of CTRWs on any time scale.

This work is structured as follows. In the next section, some general remarks are made on the definition of continuous CTRWs, Eqs. (3). Section III is dedicated to the properties of the process $t(s)$, Eq. (3b), that typically is driven by Levy noise. The numerical simulation of continuous CTRW processes is presented in Sec. IV and exemplified by means of some results in Sec. V. We conclude with Sec. VI that summarizes our results and suggests future applications.

II. CTRWS IN THE SPIRIT OF FOGEDBY: SOME REMARKS

First of all, the character of the distributions of the random variables η for the jump length and τ for the waiting time has to be addressed. In case of the discrete definition, Eqs. (1), a broad class of distributions is feasible for this purpose. The continuous Langevin formulation of Fogedby, Eqs. (3), however, requires the associated distributions to be stable in order to be properly defined. For a short introduction into the concept of stable distributions we refer to [5]. In the long-time limit, however, both approaches are equivalent.

In 1994, Fogedby introduced the stochastic differential equations (3) for CTRWs as *the continuum limit of the path parameter or arc length s along the trajectory* [12]. He considered independent random variables $\eta(s)$ and $\tau(s)$ with power-law behavior, that is,

$$\Psi(\eta,\tau) \sim \eta^{-1-\xi_\eta}\tau^{-1-\xi_\tau} \quad \text{for} \quad \eta,\tau \gg 1. \tag{4}$$

For reasons of normability, Fogedby used cutoffs at low values of $|\eta|$ and τ, respectively. He mainly was interested in the properties of the process $x(t)$ that can be obtained from Eqs. (3) by inversion of the latter process. By means of his modified power-law distributions, the long-time behavior of processes with power-law waiting jump length and waiting time distributions could be derived. In this context, first properties of the inverse process $s(t)$ of Eq. (3b) have been addressed.

Baule *et al.* investigated the properties of the inverse process $s(t)$ in greater detail [13]. In particular, multitime joint probabilities could be calculated. The waiting times τ were considered to obey one-sided Levy distributions with tail parameter α, that are discussed in greater detail in the following section. In absence of external force terms [$F=0$ in equation (3a)] analytical expressions for correlations functions could be derived by application of the inverse Fourier and Laplace transforms. Recently, these results could be extended to Ornstein-Uhlenbeck-like processes with a linear repelling term, thus $F(x)=-\gamma x$ [15].

Both works, however, focus on the ensemble statistics, whereas the Langevin approach of Fogedby, that is interesting itself, has not attracted much attention yet.

III. PROPERTIES OF $t(s)$ AND ITS INVERSE PROCESS $s(t)$

In this section we concentrate on the process $t(s)$. Due to causality, this process has to be strictly monotonically increasing. The increments $dt(s)=t(s+ds)-t(s)$, therefore, have to obey fully skewed stable distributions.

Generally, stable distributions are assigned to the α-stable probability distribution functions (PDFs). α-stable Levy distributions typically are not available in a closed form but are only accessible by means of their Fourier transform. We especially consider the distribution

$$L_\alpha(x) = \frac{1}{\pi}\,\mathrm{Re}\left\{\int_0^\infty dz\,\exp\left[-ikx - z^\alpha \exp\left(-i\frac{\alpha\pi}{2}\right)\right]\right\}. \tag{5}$$

Here, i is the imaginary unit and $0<\alpha\leq 1$ the stability index that specifies the asymptotic behavior $L_\alpha(x)\sim x^{-(1+\alpha)}$ at $x\gg 1$. This PDF complies with a common parametrization of α-stable PDFs [5,16,17],

$$L_\alpha^{\beta,c}(x) = \frac{1}{2\pi}\int_{-\infty}^{\infty} dz\,\exp\left[-ikx - cz^\alpha\left(1 - i\beta\frac{z}{|z|}\tan\frac{\alpha\pi}{2}\right)\right], \tag{6}$$

for the parameters $\beta=1$ and $c=\left(1+\tan^2\frac{\alpha\pi}{2}\right)^{(-1/2)}$. Some examples for this distribution are depicted in Fig. 1. An important feature of this representation is, according to Eq. (5), is defined even for $\alpha=1$ by means of $L_{\alpha=1}(x)=\delta(x-1)$. From the theory of stable processes it follows that the increment dt has to obey the distribution $ds^{-\alpha}L_\alpha(dt/ds^\alpha)$ [16]. The case $\alpha=1$ with $dt=ds$ complies with stochastic processes that solely can be described by Eq. (3a) with $s=t$.

An intrinsic feature of Levy processes is that trajectories contain finite jumps in terms of discontinuities with a probability greater than zero. They are continuous only from the right [18], that is,

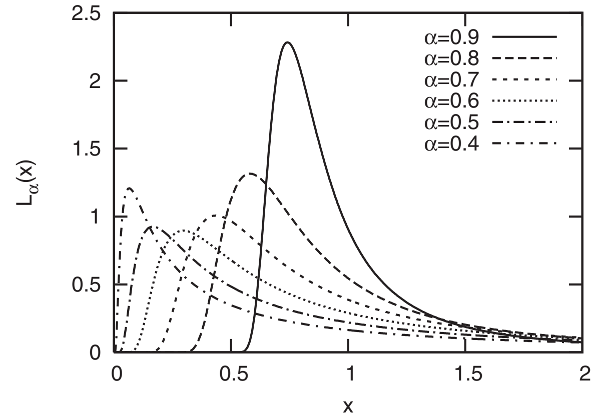

FIG. 1. Examples for the fully skewed Levy distribution according to Eq. (5) for different characteristic exponents α. For $\alpha\to 1$, the PDF converges to $\delta(x-1)$.

$$\lim_{\Delta s\to 0} t(s+\Delta s) = t(s). \tag{7}$$

A sample of a fully skewed Levy process with characteristic exponent $\alpha=0.9$ is depicted in the upper panel of Fig. 2. Due to these jumps, the range of values $t(s)$ does not cover the full interval $[0,\infty[$. Rather, the range can be specified by

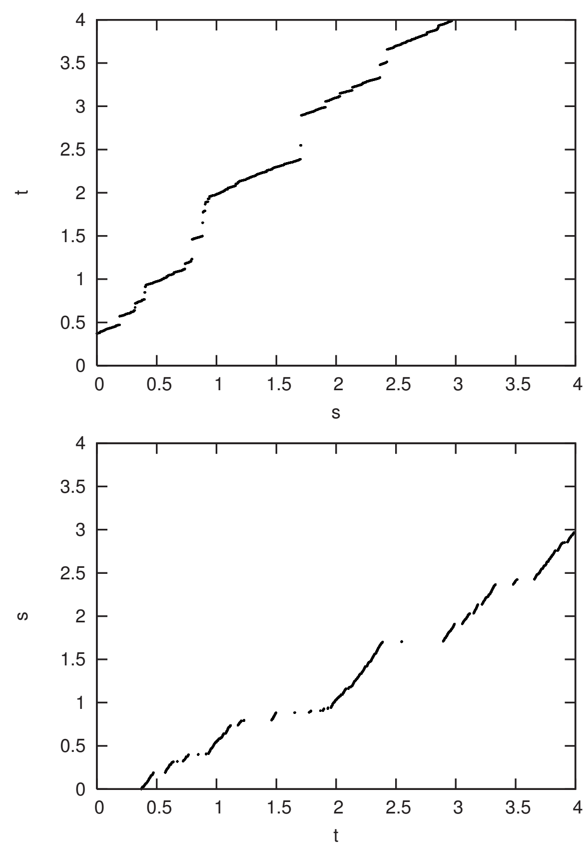

FIG. 2. Trajectories of the process $t(s)$ (upper panel) and the associated inverse process $s(t)$ (lower panel) simulated for $\alpha=0.9$. The finite jumps of the process $t(s)$ that are characteristic for Levy processes are evident. Due to these jumps the inverse process $s(t)$, however, *a priori* is not defined on $[0,\infty[$.

means of a set of intervals. Due to the monotonic increase of the process $t(s)$ a inverse process $s(t)$ exists. This process has been applied for construction of the process $x(t)=x(s(t))$ in the past. It, however, *a priori* is not properly defined for $t \in [0,\infty[$ due to the jump characteristic of the Levy process. A sample of the inverse process is depicted in the lower panel of Fig. 2.

In general, the meaning of the inverse function has to be specified in order to be properly defined on $t \in [0,\infty[$. Appropriate definitions for the inverse function, e.g., are [18]

$$s(t) \coloneqq \inf\{s{:}t(s) \geq t\} \quad \text{or} \tag{8a}$$

$$s(t) \coloneqq \sup\{s{:}t(s) \leq t\}. \tag{8b}$$

If the process $x(s)$ is steady, these definitions are equivalent in the limit $\Delta s \to 0$ for $t \in [0,\infty[$. Since $x(s)$ is steady,

$$\lim_{\Delta s \to 0} x(s-\Delta s) = \lim_{\Delta s \to 0} x(s+\Delta s) = x(s) \tag{9}$$

is valid by definition. Due to the monotonic character of the process $t(s)$, $t(s) \leq t(s+\Delta s)$ for $\Delta s \geq 0$. Consequently, $s \leq s(t') \leq s+\Delta s$ if $t(s) \leq t' \leq t(s+\Delta s)$. Then,

$$\lim_{\Delta s \to 0} x(s) = x(s(t')) = x(s+\Delta s) \tag{10}$$

is valid for $t(s) \leq t' \leq t(s+\Delta s)$. Here, for the process $t(s)$, only the continuity from the right has been used. For steady processes $x(s)$ in the limit of infinitesimal Δs, no additional definition for proper interpretation of the inverse function is required.

If unsteady jumps of $x(s)$ coincide with those of $t(s)$, the latter argumentation is not feasible. We, however, restrict ourselves to stochastic processes $x(s)$ with Gaussian noise that are steady with probability 1 for $s \in [0,\infty[$.

IV. NUMERICAL SIMULATION OF SAMPLE PATHS

An equivalent formulation of Eqs. (3) is given by the integral equations

$$x(s) = x(0) + \int_0^s ds' F(x(s')) + \int_0^s dW(s'), \tag{11a}$$

$$t(s) = t(0) + \int_0^s dL_\alpha(s'), \tag{11b}$$

where dW and dL_α are the infinitesimal increments of Wiener and α-stable Levy processes, respectively. For numerical integration these equations have to be discretisized with an adequate discrete increment Δs. Application of the Euler scheme for numerical evaluation of Eqs. (11) then yields

$$x(s+\Delta s) = x(s) + \Delta s F(x(s)) + \eta(s,\Delta s), \tag{12a}$$

$$t(s+\Delta s) = t(s) + \tau_\alpha(s,\Delta s). \tag{12b}$$

Here, the random variables $\eta(s_i,\Delta s)$ independently have to be drawn from a Gaussian PDF with variance $\sigma^2=\Delta s$. The variables $\tau_\alpha(s_i,\Delta s)$ have to comply with the distribution $\frac{1}{\Delta s^\alpha} L_\alpha\left(\frac{\tau_\alpha}{\Delta s^\alpha}\right)$. The efficient numerical generation of these random numbers is addressed in the Appendix. Due to the absence of forcing and the purely additive character of the noise, the integration of $t(s)$ by means of the Euler scheme is exact. For numerical integration of the process $x(s)$ with Gaussian noise, alternatively advanced discretization schemes can be applied [19].

For numerical simulation of trajectories $x(t)$ at discrete times $t_j \coloneqq j\Delta t$, $j=0,\ldots,N$, the inverse $s(t)$ does not have to be calculated explicitly. Instead, the following algorithm can be applied that incorporates definition (8a) for the inverse process:

(A) Initialization of $x_s(0)$ and $t_s(0)$, set $s=0$.
(B) For every $j=0$ to N,
(1) while $[t_s(s) < t_j]$
(a) calculate $x_s(s+\Delta s)$ and $t_s(s+\Delta s)$ from Eqs. (12),
(b) increase s by Δs;
(2) set $x(t_j) \coloneqq x_s(s)$.

The discretization of t, Δt, is given by the desired sampling rate of the simulated process. The optimal value for the discretization of the intrinsic variable s, Δs, depends on characteristic length scales of the process $x(s)$ and the desired accuracy of the resulting process $x(t)$. Typically, Δs has to be adjusted such that the right-hand-side term of the discrete equation, $\Delta s F(x(s_i)) + \eta(s_i,\Delta s)$, with a sufficient probability, is less than the desired accuracy of the simulation. This argument is illustrated within the scope of the following section. Too small values for Δs, in turn, may bias the accuracy of the numerical evaluation of Eqs. (12) due to discretization errors and reduce the speed of the algorithms. The choice for Δs therefore is a tradeoff between the accuracy of the discretization, validity of the inversion of the process $t(s)$, computer time, and discretization errors. For details concerning the numerical evaluation of the discretized equations (12), the reader is referred to Kloeden and Platen [19].

V. EXAMPLES

For exemplification of the simulation procedure and characteristic properties of continuous CTRWs, processes with $F(x)=-x$ are considered. The process $x(s)$ then is an ordinary Ornstein-Uhlenbeck process

$$dx(s) = -\gamma x dt + \sqrt{D} dW(s) \tag{13}$$

with $D=\gamma=1$. For later comparison with analytical results, $x(0)=1$ is used as the starting value for the process $x(s)$.

For Ornstein-Uhlenbeck processes, joint PDFs for finite time increment can be calculated in a closed form [4]. Then, the statistics of the increments $\Delta x \coloneqq x(s+\Delta s)-x(s)$ can be considered as a function of the discretization Δs. The distribution of Δx as a function Δs is Gaussian with variance

$$\langle(\Delta x)^2\rangle = 2(1-e^{-\Delta s}). \tag{14}$$

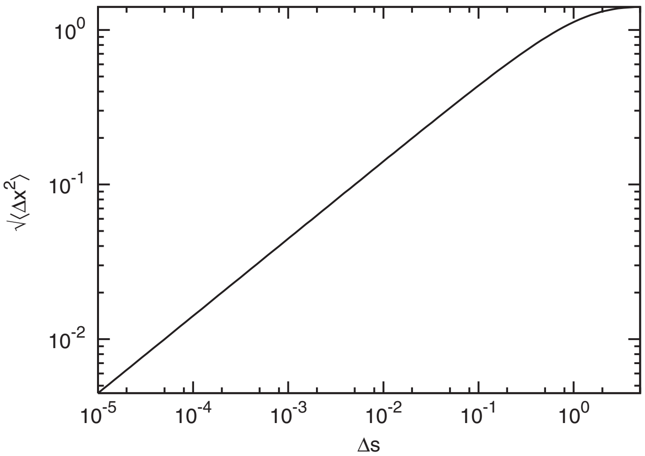

FIG. 3. Determination of the intrinsic increment Δs. From the transition PDF of Ornstein-Uhlenbeck processes that is available in a closed form, the square root of the means square deviation of the increment Δx as function of the increment Δs can be derived. From inspection of this graph, $\Delta s = 0.0001$ seems to be sufficient for the current purpose.

In order to estimate an appropriate value for Δs, the root mean square deviation has been investigated. From the inspection of Fig. 3, $\Delta s = 0.0001$ has been selected for the application in the numerical procedure. The maximum deviation of the definitions (8) from one another is $\sim 10^{-2}$, which is accurate enough for the current purpose.

10 000 data points with time increment $\Delta t = 0.001$ have been generated for several values of α. The trajectories of the respective processes are exhibited in Fig. 4. From the sample paths, the influence of the subordinating process $t(s)$ on the dynamics becomes evident. For $\alpha = 1$ an Ornstein-Uhlenbeck process is recovered. With decreasing α waiting events start to dominate the process. This also can be seen from the evolution of the increment PDFs that is depicted in Fig. 5.

Recently, the fractional extension of Ornstein-Uhlenbeck processes has been investigated by Baule *et al.* [15], starting from the fractional Fokker-Planck equation for the time evolution of ensembles of particles. For the Ornstein-Uhlenbeck process $x(s)$ with initial value $x(0) = 1$ that has been considered in this section, for $t_2 > t_1$, eventually an analytical expression for the correlation function could be derived,

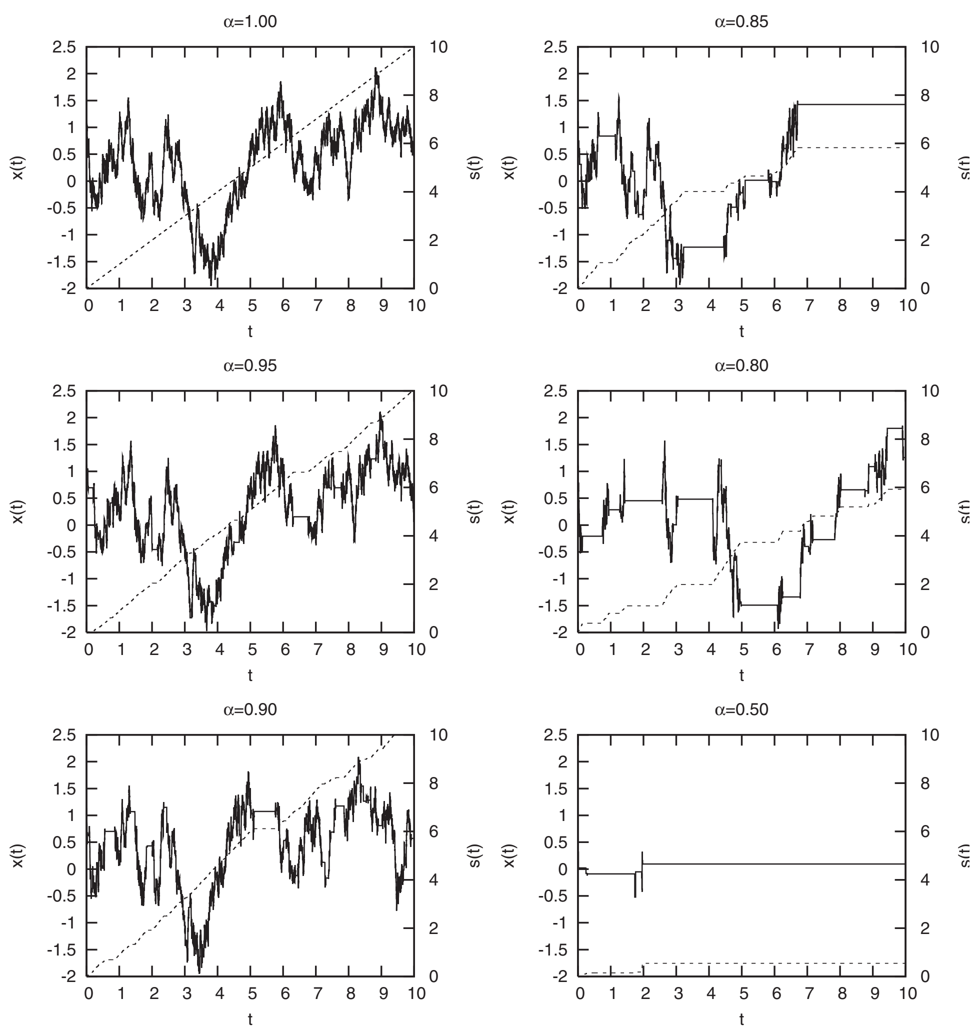

FIG. 4. Sample trajectories of CTRWs with linear repelling force $F(x) = -x$ for different stability indices α. The solid line corresponds to the process $x(t)$ whereas the dashed line indicates the corresponding $s(t)$. $\alpha = 1$ complies with the ordinary Ornstein-Uhlenbeck process. With decreasing α the process is dominated by waiting events indicated by constants x and s.

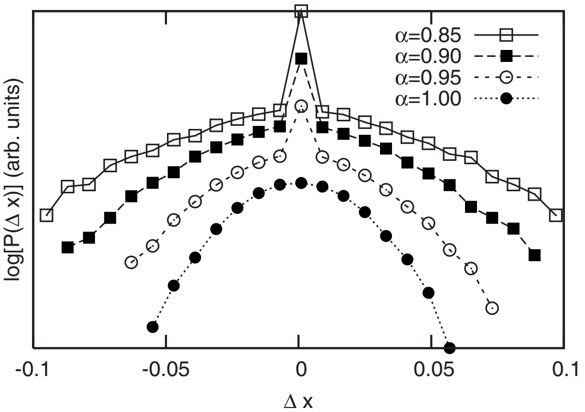

FIG. 5. Increments distributions for $\Delta x := x(t+\tau)-x(t)$ with $\tau = 0.001$ for some processes depicted in Fig. 4. For reasons of clearness the individual PDFs are shifted in vertical direction by a constant factor. It is evident that with decreasing stability index α a central peak evolves that corresponds to persistent regions due to waiting events. On the other hand, the distributions broaden indicating a higher probability of the occurrence of extreme increments.

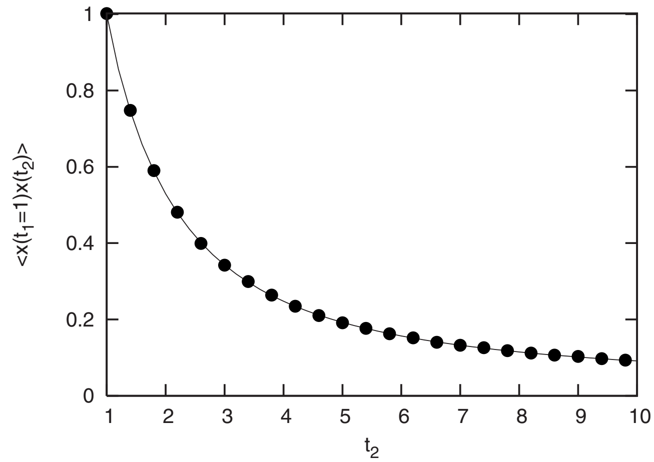

FIG. 6. Correlation function of the process depicted in Fig. 4 for $\alpha=0.8$. The solid line marks the analytical solution (15) derived by Baule *et al.* [15]. The circles indicate the correlation obtained from the analysis of an ensemble of 500 000 trajectories. Since a perfect coincidence is observed, this evaluation is proposed as a benchmark for accuracy of the numerical implementation.

$$\langle x(t_2)x(t_1)\rangle = \frac{t_1^\alpha}{\Gamma(\alpha+1)}\sum_{n=0}^{\infty}\frac{(-t_2^\alpha)^n}{\Gamma(\alpha n+1)} \times {}_2F_1\left(\alpha,-\alpha n,\alpha+1;\frac{t_1}{t_2}\right) + E_\alpha(-t_2^\alpha). \quad (15)$$

Here, Γ denotes the Gamma function, E_α the one-parameter Mittag-Leffler function, and ${}_F2_1(a,b,c;z)$ the Gaussian hypergeometric function. For details see the references provided by Baule *et al.* [15].

On the other hand, the correlations can be estimated from ensemble averages of simulated trajectories $x(t)$. A comparison of the analytical result by Baule *et al.* with the correlations estimated from our simulated trajectories is exhibited in Fig. 6. Perfect coincidence of these two approaches is observed that never could be compared before.

VI. SUMMARY AND CONCLUSIONS

A method for the accurate and efficient simulation of continuous trajectories of continuous-time random walk (CTRW) processes has been proposed that relies on the representation through Langevin equations proposed by Fogedby. It is based on the simultaneous simulation of two stochastic processes, one of which is driven by Levy noise.

Within the scope of Sec. III, the construction of the process $x(t)=x(s(t))$ with the aid of the inverse $s(t)$ of the Levy process $t(s)$ has been discussed in great detail. The unique existence of the inverse of $t(s)$ for any t typically has been assumed in the past [13]. However, the meaning of the inverse process in fact has to be specified in detail at discontinuities of $t(s)$ in order to guarantee for unique existence, see, e.g., Eqs. (8). We would like to emphasize that these additional specifications influence neither the trajectories $x(t)$ nor the ensemble statistics if the trajectories $x(s)$ are continuous with probability 1. In the subsequent sections, we mainly focussed on this specific case.

Comparison with recent analytical results by Baule *et al.* [15] has been used for validation of the simulation procedure and showed compliance of the results. Due to the non-Markovian character of fractional processes, higher-order joint statistics are of great interest [20]. We propose the use of probabilistic methods for numerical calculation of these functions.

ACKNOWLEDGMENTS

The authors kindly acknowledge intensive discussions with Adrian Baule, Stephan Eule, Michael Wilczek, and Eli Barkai. Adrian Baule provided the numerical evaluation of Eq. (15) that has been used in Fig. 6 for comparison with our numerical results. Financial support was granted by the Bundesministerium für Bildung, Forschung und Wissenschaft (BMBF) within the project Windturbulenzen und deren Bedeutung für die Windenergie.

APPENDIX: GENERATION OF RANDOM VARIABLES WITH SKEWED α-STABLE PDF ACCORDING TO EQ. (5)

Skewed Levy-stable random numbers efficiently can be generated by means of the algorithm proposed in [16,17]. We adapted this algorithm to our definition of the skewed Levy distributions, Eq. (5).

The random numbers $\tau_\alpha(s_i,\Delta s)$ are required for numerical integration of the process $t(s)$, then for $0<\alpha\leq 1$ efficiently can be generated by means of the following algorithm:

(i) Generate a random variable V_i uniformly distributed on $]-\pi/2,\pi/2[$ and an independent exponential random variable W_i with mean 1. Several optimized random number generators are available for this purpose. In case of doubt, V and W can be obtained from two independent variables u_i^1 and u_i^2 that are uniformly distributed on $]0,1[$ by means of

$$V_i = \pi\left(u_i^1 - \frac{1}{2}\right), \tag{A1}$$

$$W_i = -\log(u_i^2). \tag{A2}$$

(ii) Set

$$\tau_\alpha(s_i,\Delta s) = (\Delta s)^{1/\alpha}\frac{\sin\left[\alpha\left(V_i+\frac{\pi}{2}\right)\right]}{[\cos(V_i)]^{(1/\alpha)}} \times \left\{\frac{\cos\left[V_i - \alpha\left(V_i+\frac{\pi}{2}\right)\right]}{W_i}\right\}^{(1-\alpha)/\alpha}. \tag{A3}$$

In case of $\alpha \equiv 1$, $\tau_1(s_i,\Delta s)=\Delta s$ is recovered. If adequate random-number generators are applied for the generation of the variables V_i and W_i, the resulting random-numbers τ_α are uncorrelated. From Fig. 7 it becomes evident that the desired skewed α-stable Levy PDF (5) is matched. This algorithm therefore can be applied for efficient numerical simulation of the process $t(s)$ according to Eq. (12a).

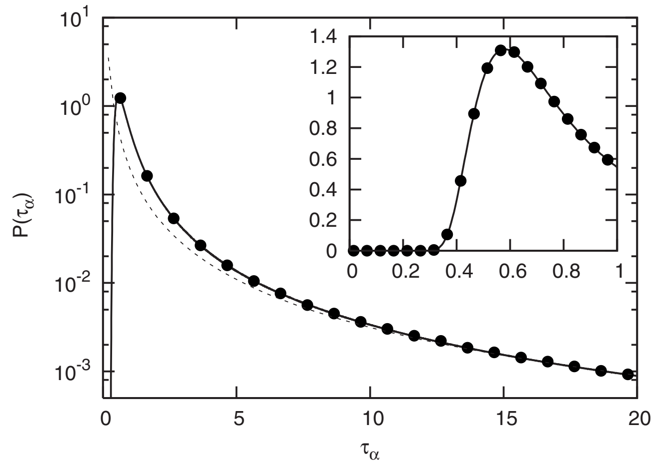

FIG. 7. Performance of the generation of skewed α-stable random numbers. The solid line exhibits the PDF obtained by numerical integration of Eq. (5) for $\alpha=0.8$. For $x \gg 1$ the PDF shows power-law decay with the exponent $1+0.8$ that is depicted dashed. The points mark the PDF obtained from a sample of 10^7 random numbers that have been generated by means of Eq. (A3) for the same stability index. The analytical PDF evidently is well reproduced by the sample of random numbers.

[1] L. Bachelier, Ann. Sci. Ec. Normale Super. **17**, 21 (1900).
[2] A. Einstein, Ann. Phys. **17**, 549 (1905), reprinted in *Einstein's Annalen Papers* (Wiley-VCH Verlag, Weinheim, Germany, 2005).
[3] D. S. Lemons, *An Introduction to Stochastic Processes in Physics* (Johns Hopkins University Press, Baltimore, MD, 2002).
[4] H. Risken, *The Fokker-Planck equation*, 2nd ed., Springer Series in Synergetics Vol. 18 (Springer-Verlag, Berlin, 1989).
[5] R. Metzler and J. Klafter, Phys. Rep. **339**, 1 (2000).
[6] M. Dentz, A. Cortis, H. Scher, and B. Berkowitz, Adv. Water Resour. **27**, 155 (2004).
[7] E. W. Montroll and G. H. Weiss, J. Math. Phys. **6**, 167 (1965).
[8] J. Klafter, A. Blumen, and M. F. Shlesinger, Phys. Rev. A **35**, 3081 (1987).
[9] G. H. Weiss, *Aspects and Applications of the Random Walk* (North Holland, Amsterdam, 1994).
[10] E. Heinsalu, M. M. Patriarca, I. Goychuk, G. Schmid, and P. P. Hänggi, Phys. Rev. E **73**, 046133 (2006).
[11] R. Gorenflo, F. Mainardi, and A. Vivoli, Chaos, Solitons Fractals **34**, 87 (2007).
[12] H. C. Fogedby, Phys. Rev. E **50**, 1657 (1994).
[13] A. Baule and R. Friedrich, Phys. Rev. E **71**, 026101 (2005).
[14] A. Baule and R. Friedrich, Europhys. Lett. **77**, 10002 (2007).
[15] A. Baule and R. Friedrich, e-print arXiv:0705.4473v1.
[16] A. Janicki and A. Weron, *Simulation and Chaotic Behavior of α-Stable Stochastic Processes* (Dekker, New York, 1994).
[17] R. Weron, Int. J. Mod. Phys. C **12**, 209 (2001).
[18] M. M. Meerschaert and H.-P. Scheffler, J. Appl. Probab. **41**, 623 (2004).
[19] P. E. Kloeden and E. Platen, *Numerical Solution of Stochastic Differential Equations*, Applications of Mathematics Vol. 23 (Springer-Verlag, Berlin, 1992).
[20] E. Barkai and I. M. Sokolov, J. Stat. Mech.: Theory Exp. (2007) 08001.